



Integrity of hafnium silicate/silicon dioxide ultrathin films on Si

J. Morais, L. Miotti, G. V. Soares, S. R. Teixeira, R. Pezzi, K. P. Bastos, I. J. R. Baumvol, A. L. P. Rotondaro, J. J. Chambers, M. R. Visokay, and L. Colombo

Citation: [Applied Physics Letters](#) **81**, 2995 (2002); doi: 10.1063/1.1515112

View online: <http://dx.doi.org/10.1063/1.1515112>

View Table of Contents: <http://scitation.aip.org/content/aip/journal/apl/81/16?ver=pdfcov>

Published by the [AIP Publishing](#)

Articles you may be interested in

[Changes in the density of ultrathin silicon oxide films related to excess Si atoms near the oxide–Si\(100\) interface](#)
J. Appl. Phys. **91**, 1108 (2002); 10.1063/1.1425423

[Hafnium interdiffusion studies from hafnium silicate into silicon](#)
Appl. Phys. Lett. **79**, 4192 (2001); 10.1063/1.1425466

[Density difference related to humidity during dry oxidation for ultrathin silicon oxide films](#)
J. Appl. Phys. **86**, 5968 (1999); 10.1063/1.371641

[Structural change and heteroepitaxy induced by rapid thermal annealing of CaF₂ films on Si\(111\)](#)
J. Vac. Sci. Technol. A **16**, 2437 (1998); 10.1116/1.581363

[Density of ultradry ultrathin silicon oxide films and its correlation with reliability](#)
J. Appl. Phys. **82**, 4916 (1997); 10.1063/1.366357

A small image of the cover of an Applied Physics Reviews journal issue. The cover features a 3D diagram of a layered structure with labels for 'Substrate', 'Heterostructure', and 'Superstrate'. The AIP logo and 'Applied Physics Reviews' are at the top. The date 'apr 2012' is at the bottom left.

NEW Special Topic Sections

NOW ONLINE
Lithium Niobate Properties and Applications:
Reviews of Emerging Trends

AIP Applied Physics
Reviews

Integrity of hafnium silicate/silicon dioxide ultrathin films on Si

J. Morais, L. Miotti, G. V. Soares, S. R. Teixeira, R. Pezzi, K. P. Bastos,
and I. J. R. Baumvol^{a)}

Instituto de Física, Universidade Federal do Rio Grande do Sul, CP 15051 Porto Alegre 91501-970, Brazil

A. L. P. Rotondaro, J. J. Chambers, M. R. Visokay, and L. Colombo

Silicon Technology Development, Texas Instruments Incorporated, Dallas, Texas 75265

(Received 14 June 2002; accepted 23 August 2002)

Rapid thermal annealing at 1000 °C of $(\text{HfO}_2)_{1-x}(\text{SiO}_2)_x$ pseudobinary alloy films deposited on Si were performed in N_2 or O_2 atmospheres. The effects on the atomic transport, structure, and composition were investigated using isotopic substitution of oxygen, high-resolution transmission electron microscopy, nuclear reaction analyses, narrow nuclear reaction resonance profiling, and grazing angle x-ray reflection. © 2002 American Institute of Physics. [DOI: 10.1063/1.1515112]

There is currently an intensive search for alternative materials to replace SiO_2 or SiO_xN_y as gate dielectrics in advanced, Si-based complementary metal-oxide-semiconductor (CMOS) transistors.¹ Hafnium oxide and hafnium silicates have shown themselves to be potential candidates for an alternative gate dielectric.²⁻⁷ In order to be effectively incorporated into ultralarge scale integration (ULSI) fabrication technology, the gate dielectric material must maintain its integrity during further processing steps. In particular, rapid thermal annealing (RTA) of source and drain dopants, usually performed at and above 1000 °C, has been shown to be the most aggressive step.^{4,7} The deleterious consequences of postgate dielectric deposition annealing that have been reported so far include thickening of the SiO_2 interface layer and chemical reactions at both the gate electrode/dielectric and dielectric/substrate interfaces, with the consequent lowering of the capacitance equivalent thickness (CET).^{3,4,6,8} Furthermore, these studies pointed out the need for controlling the effects of annealing in intentionally or unintentionally O_2 -containing atmosphere (even at very low O_2 partial pressures), which renders postdeposition annealing that is even more aggressive to gate dielectric integrity, especially in the region near the dielectric-semiconductor interface.^{3,6,9-13}

We report here the effects of RTA at 1000 °C on the structure, composition, atomic transport, and oxygen incorporation kinetics in hafnium silicate films on Si. The hafnium silicate films, which are actually $(\text{HfO}_2)_{1-x}(\text{SiO}_2)_x$ pseudobinary alloys or compounds,⁴ were deposited by reactive sputtering in O_2 onto HF-cleaned, 200 mm Si(100) *p*-type substrates. RTA was performed in N_2 (N_2 annealing) and O_2 (O_2 annealing) at atmospheric pressure. RTA in O_2 was also performed in 7×10^3 Pa of O_2 97% enriched in the ^{18}O isotope ($^{18}\text{O}_2$ annealing). This allows differentiation between oxygen incorporated from the gas phase and that previously existing in the films. Samples were analyzed by cross-sectional high-resolution transmission electron microscopy (HRTEM), Rutherford backscattering spectroscopy (RBS) of He^+ ions in a channeling geometry with grazing angle detection of the scattered ions (channeled RBS),¹² nuclear reaction analysis (NRA),¹² narrow nuclear resonant reaction

profiling (NRP) of ^{18}O and ^{29}Si ,¹² and grazing angle x-ray reflection.

Cross-sectional HRTEM images of as-deposited and annealed (N_2 or O_2 , 1000 °C, 60 s) samples are shown in Figs. 1(a)–1(c). The as-deposited sample consisted of an

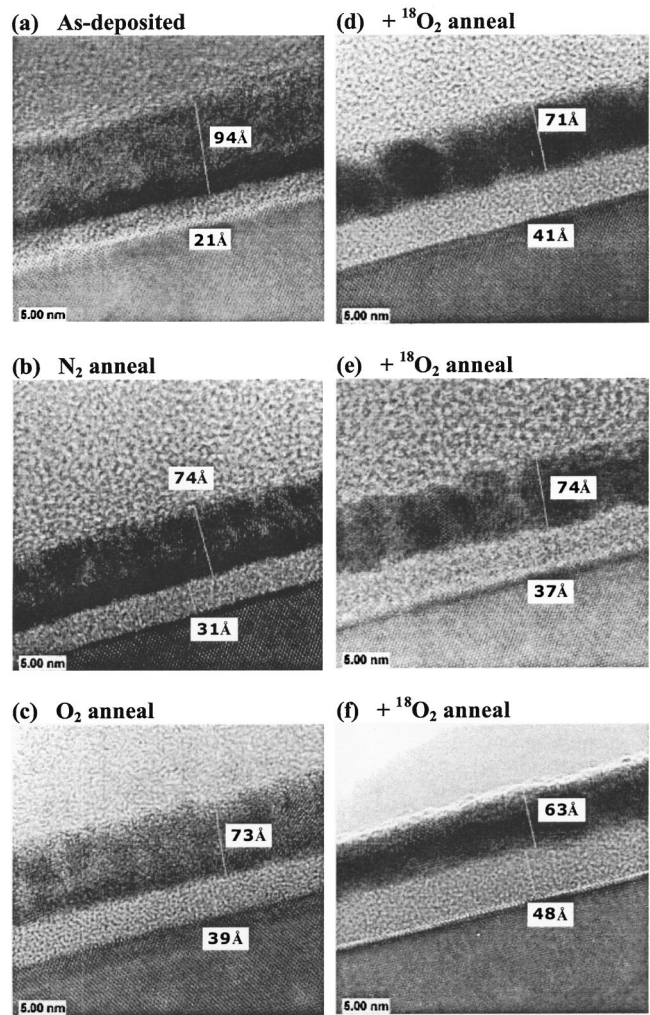


FIG. 1. Cross-sectional high-resolution transmission electron microscopy images of (a) as-deposited, (b) N_2 -annealed at 1000 °C for 60 s, (c) O_2 -annealed at 1000 °C for 60 s samples, (d) sample (a) annealed in $^{18}\text{O}_2$ at 1000 °C for 60 s, (e) sample (b) annealed in $^{18}\text{O}_2$ at 1000 °C for 60 s, and (f) sample (c) annealed in $^{18}\text{O}_2$ at 1000 °C for 60 s.

^{a)}Electronic mail: israel@if.ufrgs.br

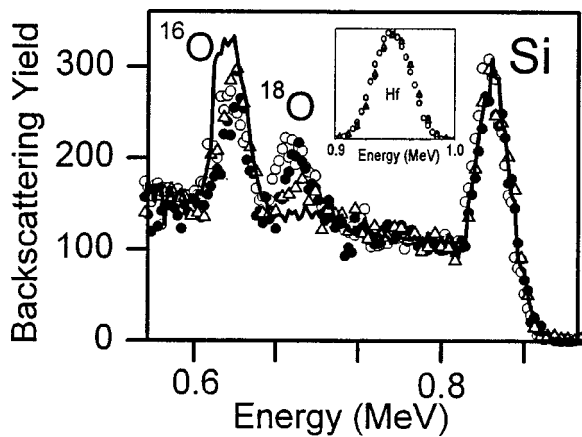


FIG. 2. Channeled-RBS spectra of 1 MeV incident He^- ions: as-deposited sample (solid line), $^{18}\text{O}_2$ annealed at 1000 °C for 60 s (open circles), O_2 annealed at 1000 °C for 60 s followed by $^{18}\text{O}_2$ annealing at 1000 °C for 60 s (closed circles), and N_2 annealed at 1000 °C for 60 s followed by $^{18}\text{O}_2$ annealing at 1000 °C for 60 s (open triangles). The corresponding Hf signals are shown in the inset.

amorphous $(\text{HfO}_2)_{1-x}(\text{SiO}_2)_x$ layer approximately 9 nm thick and an underlying 2 nm thick amorphous SiO_2 -like layer formed on the Si substrate during deposition. A transition region with distinct contrast can be observed between the $(\text{HfO}_2)_{1-x}(\text{SiO}_2)_x$ film and the SiO_2 underlayer in Fig. 1(a). N_2 annealing leads [Fig. 1(b)] to more well defined interfaces, to densification (thinning) of the $(\text{HfO}_2)_{1-x}(\text{SiO}_2)_x$ layer, and to an increase in the thickness of the SiO_2 layer. The same effects are observed following O_2 annealing, in which case a larger increase of the SiO_2 layer is observed. The samples shown in Figs. 1(a)–1(c) were subjected to further $^{18}\text{O}_2$ annealing at 1000 °C for 60 s and the corresponding cross-sectional HRTEM images are shown in Figs. 1(d)–1(f). One notices further growth of the SiO_2 interlayer, although the integrity of the $(\text{HfO}_2)_{1-x}(\text{SiO}_2)_x$ film and abruptness of the interfaces was largely maintained. In all cases, annealing produces an increase in the crystallization of the films: the TEM images of Figs. 1(d) and 1(e) suggest some microstructural instability after annealing as well.

The elemental composition of the as-deposited samples was determined by RBS and NRA to be approximately HfSi_2O_5 , which remained essentially the same after RTA annealing in N_2 and O_2 . Channeled-RBS spectra of 1 MeV incident He^+ ions from the as-deposited and $^{18}\text{O}_2$ -annealed samples shown in Fig. 1 are displayed in Fig. 2. One notices the immobility of Hf and the incorporation of ^{18}O from the gas phase into the $(\text{HfO}_2)_{1-x}(\text{SiO}_2)_x/\text{SiO}_2$ film structure. Previous work revealed that Hf from hafnium silicate is much less likely to penetrate Si than other studied cases like, for example, Zr from zirconium silicate.^{9,10}

^{18}O profiles in these samples were determined by NRA using the $^{18}\text{O}(p,\alpha)^{15}\text{N}$ nuclear reaction around the resonance at 151 keV ($\Gamma_R=100$ eV). Excitation curves and extracted ^{18}O profiles¹² are shown in Fig. 3(a). One can see that oxygen from the gas phase diffuses from the surface and reacts with the hafnium silicate network. According to Fig. 2, ^{16}O – ^{18}O exchange is probably the main reaction channel. However, since the total amount of oxygen ($^{16}\text{O}+^{18}\text{O}$) was found to increase during annealing, other reaction channels

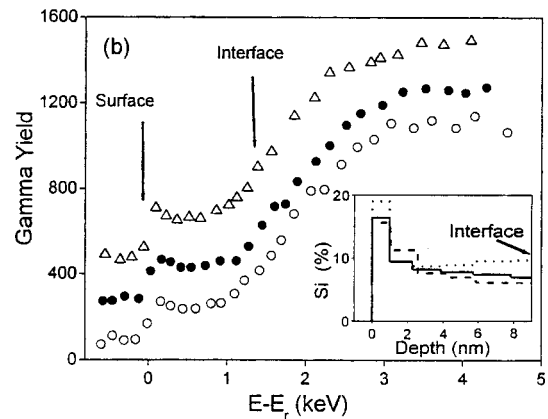
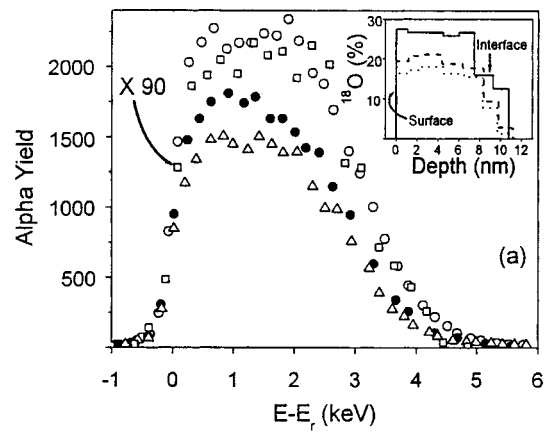


FIG. 3. (a) Excitation curves of the $^{18}\text{O}(p,\alpha)^{15}\text{N}$ nuclear reaction around the resonance at 151 keV with the corresponding ^{18}O profiles in the inset: as-deposited sample (open squares, $\times 90$), $^{18}\text{O}_2$ annealed at 1000 °C for 60 s (open circles, solid line), O_2 annealed at 1000 °C for 60 s followed by $^{18}\text{O}_2$ annealing at 1000 °C for 60 s (closed circles, dashed line), N_2 annealed at 1000 °C for 60 s followed by $^{18}\text{O}_2$ annealing at 1000 °C for 60 s (open triangles, dotted line). (b) Excitation curves of the $^{29}\text{Si}(p,\gamma)^{31}\text{P}$ nuclear reaction around the resonance at 414 keV with the corresponding ^{29}Si profiles in the inset with the same symbols as in (a).

must be active, such as completion of the silicate stoichiometry and oxidation of the Si substrate. Samples that were pre-annealed in either O_2 or N_2 are more resistant to the propagation of the ^{18}O front than the as-deposited one. Therefore, less ^{18}O will reach and oxidize the Si substrate in the pre-annealed samples than in the as-deposited one, consistent with the HRTEM images of Fig. 1. ^{29}Si profiles were determined in the $^{18}\text{O}_2$ -annealed samples using the $^{29}\text{Si}(p,\gamma)^{30}\text{P}$ nuclear reaction around the resonance at 414 keV ($\Gamma_R \approx 100$ eV). Excitation curves and the profiles extracted are shown in Fig. 3(b), where one notices an accumulation of Si at the film surfaces and a roughly constant Si concentration in the bulk of the as-deposited sample. Si remained essentially immobile during 1000 °C annealing, different from several previously studied materials.^{9,13–17}

Thus, oxygen reaction diffusion is a significant atomic scale concern with regard to the instability of the $(\text{HfO}_2)_{1-x}(\text{SiO}_2)_x/\text{SiO}_2/\text{Si}$ system. It has to be controlled before hafnium silicate films can be seriously considered as replacements for SiO_2 or SiO_xN_y as the gate dielectric. In order to further investigate this aspect, the kinetics of ^{18}O incorporation during RTA of the as-deposited film at 1000 °C in $^{18}\text{O}_2$ were determined by NRA. The result is shown in Fig. 4(a). For annealing times up to 30 s, a duration that would be

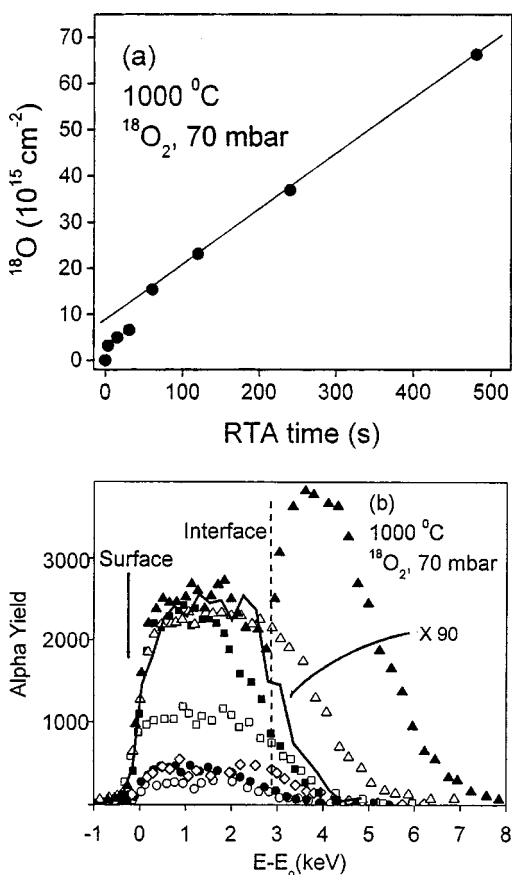


FIG. 4. (a) Kinetics of ^{18}O incorporation during RTA in $^{18}\text{O}_2$ at $1000\text{ }^\circ\text{C}$ of the as-deposited film determined by nuclear reaction analysis. (b) Excitation curves of the $^{18}\text{O}(p, \alpha)^{15}\text{N}$ nuclear reaction around the resonance at 151 keV for 3 (open circles), 15 (closed circles), 30 (open diamond), 60 (open squares), 120 (closed squares), 240 (open triangles), and 480 s (closed triangles). The solid line represents the excitation curve for the as-deposited sample ($\times 90$).

sufficient for most dopant annealing processing steps, the ^{18}O incorporation is fairly moderate. Furthermore, excitation curves of the $^{18}\text{O}(p, \alpha)^{15}\text{N}$ nuclear reaction around the resonance at 151 keV shown in Fig. 4(b) indicate that, for 30 s annealing, the ^{18}O front barely reaches the dielectric/substrate interface and thus only minor oxidation of the Si substrate is expected. For 60 s annealing time there is an abrupt increase in ^{18}O incorporation which is accompanied by a substantial part of the ^{18}O propagating front reaching the dielectric/substrate interface, leading to large thickening of the SiO_2 interlayer as shown in Fig. 1(a). The ^{18}O concentration in the $(\text{HfO}_2)_{1-x}(\text{SiO}_2)_x$ film reaches saturation at approximately 30%, after which only the propagation of the ^{18}O front in depth is observed. For the longest RTA time, 480 s, the excitation curve exhibits a distinct zone towards higher values of $E-E_R$ with a much higher concentration of ^{18}O . The ^{18}O profile extracted reveals that this is a Si^{18}O_2 layer, approximately 5 nm thick, that has formed beneath the $(\text{HfO}_2)_{1-x}(\text{SiO}_2)_x/\text{SiO}_2$ thin film structure by reaction of diffusing $^{18}\text{O}_2$ (or ^{18}O)¹³ with the Si substrate. This aggressive annealing in oxygen causes dramatic changes in the thickness and abruptness of the interfaces as is shown in the x-ray reflectivity results in Fig. 5.

In summary, compared to previous materials considered

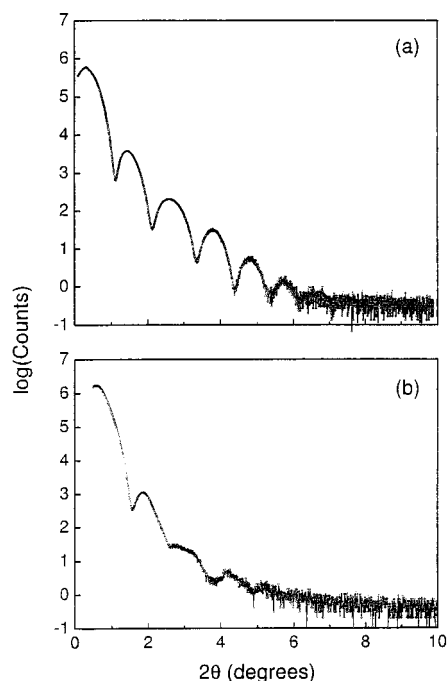


FIG. 5. Grazing-angle x-ray reflection from a sample (a) as deposited and (b) $^{18}\text{O}_2$ annealed at $1000\text{ }^\circ\text{C}$ for 480 s.

as SiO_2 replacements as the gate dielectric, such as Al_2O_3 , ZrO_2 , Zr-Si-O , Zr-Al-O , Gd_2O_3 , Gd-Si-O , and others, the present hafnium silicate films present higher stability against annealing at $1000\text{ }^\circ\text{C}$.

- ¹ *International Technology Roadmap for Semiconductors* (Semiconductor Industry Association International, San Jose, CA, 2000).
- ² B. K. Park, J. Park, M. Cho, C. S. Hwang, K. Oh, Y. Han, and D. Y. Yang, *Appl. Phys. Lett.* **80**, 2368 (2002).
- ³ A. Callegari, E. Cartier, M. Gribelyuk, H. F. Okorn-Schmidt, and T. Zabel, *J. Appl. Phys.* **90**, 6466 (2001).
- ⁴ G. D. Wilk, R. M. Wallace, and J. M. Anthony, *J. Appl. Phys.* **89**, 5243 (2001); **87**, 484 (2000).
- ⁵ S. A. Campbell, T. Z. Ma, R. Smith, W. L. Gladfelter, and F. Chen, *Microelectron. Eng.* **59**, 361 (2001).
- ⁶ K.-J. Choi, W.-C. Shin, and S.-G. Yoon, *J. Electrochem. Soc.* **149**, F18 (2002).
- ⁷ M. R. Visokay, J. J. Chambers, A. L. P. Rotondaro, A. Shanware, and L. Colombo, *Appl. Phys. Lett.* **80**, 3183 (2002).
- ⁸ J. Park, B. K. Park, M. Cho, C. S. Hwang, K. Oh, and D. Y. Yang, *J. Electrochem. Soc.* **149**, G89 (2002).
- ⁹ M. Quevedo-Lopez, M. El-Bouanani, S. Addepalli, J. L. Duggan, B. E. Gnade, M. R. Visokay, M. Douglas, M. J. Bevan, and L. Colombo, *Appl. Phys. Lett.* **79**, 2958 (2001).
- ¹⁰ M. Quevedo-Lopez, M. El-Bouanani, S. Addepalli, J. L. Duggan, B. E. Gnade, R. M. Wallace, M. R. Visokay, M. Douglas, and L. Colombo, *Appl. Phys. Lett.* **79**, 4192 (2001).
- ¹¹ B. H. Lee, L. Kang, R. Nieh, W.-J. Qi, and J. C. Lee, *Appl. Phys. Lett.* **76**, 1926 (2000).
- ¹² I. J. R. Baumvol, *Surf. Sci. Rep.* **36**, 1 (1999), and references therein.
- ¹³ B. W. Busch, W. H. Schulte, E. Garfunkel, T. Gustafsson, W. Qi, R. Nieh, and J. Lee, *Phys. Rev. B* **62**, 13290 (2000).
- ¹⁴ D. Landheer, X. Wu, J. Morais, I. J. R. Baumvol, R. P. Pezzi, L. Miotti, W. N. Lennard, and J. K. Kim, *Appl. Phys. Lett.* **79**, 2618 (2001).
- ¹⁵ M. Kundu, N. Miyata, and M. Ichikawa, *Appl. Phys. Lett.* **78**, 1517 (2001).
- ¹⁶ C. Krug, E. B. O. da Rosa, R. C. M. de Almeida, J. Morais, I. J. R. Baumvol, T. D. M. Salgado, and F. C. Stedile, *Phys. Rev. Lett.* **86**, 4714 (2001); see also M. Copel, *ibid.* **86**, 4713 (2001).
- ¹⁷ J. Morais, E. B. O. da Rosa, L. Miotti, R. P. Pezzi, I. J. R. Baumvol, A. L. P. Rotondaro, M. J. Bevan, and L. Colombo, *Appl. Phys. Lett.* **78**, 2446 (2001).